23. J. Winderickx *et al.*, *Hum. Mol. Genet.* **2**, 1413 (1993).
24. Genomic DNA can be isolated from many tissues. However, because only eye tissue has survived, this was used for the amplification of opsin genes by PCR. Small pieces of the dry eye tissue of not more than 1 mm^3 were placed in 0.2-ml eppendorf tubes, and 20 μl of GeneReleaser (BioVentures) was added. GeneReleaser serves two purposes: It avoids the need to purify DNA, and it sequesters products that might inhibit polymerase activity. The tube was heated as follows: 65°C for 30 s, 8°C for 30 s, 97°C for 180 s, 8°C for 60 s, 65°C for 180 s, 97°C for 60 s, 65°C for 60 s, and 80°C for 1 hour. The PCR mix was then either added immediately or after storage at 4°C overnight. The PCR mix contained 200 μM each of 2′-deoxyadenosine 5′-triphosphate, deoxycytidine 5′-triphosphate, deoxyguanosine 5′-triphosphate, and deoxythymidine 5′-triphosphate, 0.5 units of *Taq* polymerase, 9 mM $MgCl_2$, 30 μM of each primer, and 2 μl of Perfect Match (Stratagene), all in a final volume of 50 μl. The tube was heated at 94°C for 180 s before 35 cycles of 94°C for 20 s, 62°C for 30 s, and 72°C for 120 s, and a final step of 72°C for 600 s. No products of this first round of PCR could be visualized on an agarose gel. A second round of PCR was then carried out by the addition of 1 μl of the first-round mix to 49 μl of PCR mix prepared as before but preheated to 94°C. The PCR parameters were as for the first round except that the annealing temperature was adjusted as follows: R4+, R5– and G4+, G4– at 62°C; E3+, E3– and E4+, E4– at 56°C; E5+, E5– at 58°C; and I4+, I5– at 68°C. Blank tubes lacking DNA were carried through both first- and second-round PCRs. No amplified fragments were detected in these tubes. The test DNA samples from a normal male observer, an anomalous male trichromat, and a male deuteranope were isolated by conventional methods from blood samples, and only a single PCR was carried out with the parameters of the second-round PCR.
25. The sequence of the two sets of primer oligonucleotides used for the amplification of the opsin gene fragments are as follows. (i) Gene-specific set: R4+, GCTGCATCATCCCACTCGC; G4+, GCTGCATCACCCCACTCAG; R5–, GACGCAGTACGCAAAGATC; and G5–, GAAGCAGAATGCCAGGACC. (ii) Nonspecific set: E3+, TCACAGGTCTCTGGTCTCTGG; E3–, CTCCAACCAAAGATGGGCGG; E4+, CACGGCCTGAAGACTTCATGC; E4–, CGCTCGGATGGCCAGCCACAC; E5+, GAATTCCACCCAGAAGGCAGAG; E5–, GTCGACGGGGTTGTAGATAGTGGC; I4+, ACGTGGAATTCCCTCTCCTCCTCCCCACAAC; and I5–, ACGTGAAGCTTCAGGTGGGGCCATCACTGCA.
26. S. S. Deeb *et al.*, *Am. J. Hum. Genet.* **51**, 687 (1992).
27. K. S. Dulai, J. K. Bowmaker, J. D. Mollon, D. M. Hunt, *Vision Res.* **34**, 2483 (1994).
28. J. Nathans *et al.*, *Am. J. Hum. Genet.* **53**, 987 (1993).
29. Amplified fragments for sequencing were obtained from excised gel bands of the correct size by eluting the fragments from the bands overnight in 50 μl of sterile water and then heating the fragments to 68°C for 5 min. After TA cloning (Invitrogen) into pCRII, the fragments were cycle-sequenced with *Taq* polymerase, dye-tagged dideoxy nucleotides, and either a T7 or Sp6 sequencing primer. The products of the reaction were visualized in an Applied Biosystems Model 373 DNA Sequencer System.
30. E. Hagelberg, I. C. Gray, A. J. Jeffreys, *Nature* **352**, 427 (1991).
31. W. D. Wright, *The Rays Are not Coloured* (Hilger, London, 1967).
32. D. Brewster, *Letters on Natural Magic, Addressed to Sir Walter Scott, Bart* (J. Murray, London, 1842).
33. E. Wartmann, *Taylor's Sci. Mem.* **4**, 156 (1846).
34. A. Kohlrausch, *Pfluegers Arch. Gesamte Physiol. Menschen Tiere* **200**, 216 (1923).
35. G. Wyszecki and W. S. Stiles, *Color Science* (Wiley, New York, 1982).
36. Supported by the Wellcome Trust and the Medical Research Council. We thank the Manchester Literary and Philosophical Society for permission to take samples from Dalton's eye; the Museum of Science and Industry in Manchester for giving us access to their material; H. Key for the provision of a specimen of *P. zonale*; D. Hull, C. James, H. Key, E. Spong, and E. N. Willmer for botanical advice; I. Cannell for photography; and the Director of the Botanic Garden and the Keeper of Manuscripts, Cambridge University, for access to colorimetric samples.

RESEARCH ARTICLE

Mechanism of Inhibition of HIV-1 Reverse Transcriptase by Nonnucleoside Inhibitors

Rebecca A. Spence, Warren M. Kati, Karen S. Anderson, Kenneth A. Johnson*

The mechanism of inhibition of HIV-1 reverse transcriptase by three nonnucleoside inhibitors is described. Nevirapine, O-TIBO, and Cl-TIBO each bind to a hydrophobic pocket in the enzyme-DNA complex close to the active site catalytic residues. Pre–steady-state kinetic analysis was used to establish the mechanism of inhibition by these noncompetitive inhibitors. Analysis of the pre–steady-state burst of DNA polymerization indicated that inhibitors blocked the chemical reaction, but did not interfere with nucleotide binding or the nucleotide-induced conformational change. Rather, in the presence of saturating concentrations of the inhibitors, the nucleoside triphosphate bound tightly (K_d, 100 nM), but nonproductively. The data suggest that an inhibitor combining the functionalities of a nonnucleoside inhibitor and a nucleotide analog could bind very tightly and specifically to reverse transcriptase and could be effective in the treatment of AIDS.

Virally encoded human immunodeficiency virus (HIV) reverse transcriptase (RT) catalyzes the replication of single-stranded viral RNA to yield double-stranded DNA before the viral genome is integrated into the DNA of the host. RT has been the target of several antiviral therapeutic agents (*1*) used in the treatment of AIDS. Although nucleoside analogs, such as AZT (3′-azido 3′-deoxythymidine) and ddC (2′,3′-dideoxycytidine), have been the drugs of choice in attenuating the action of the virus, toxicity limits their use (*2*) and long-term inhibition of RT is limited by the high frequency of virus mutation whereby drug-resistant forms may accumulate (*3*). In searches for new inhibitors, random screening has resulted in the identification of several classes of nonnucleoside RT inhibitors. These include the tetrahydro-benzodiazepine (TIBO) derivatives and the dipyridodiazepinone Nevirapine (*4*–*6*) (Fig. 1). Because the nonnucleoside derivatives inhibit RT at low concentrations and with high specificity, these inhibitors are promising candidates for the treatment of AIDS. However, as in the case of the nucleoside analogs (*3*, *7*), TIBO- and Nevirapine-resistant forms of RT have already been identified (*8*, *9*). Several studies undertaken in an effort to retard the onset of resistance have been focused on convergent combination therapy (*2*, *10*).

A crystal structure of RT with Nevirapine bound shows the inhibitor in a hydrophobic pocket near the polymerization active site (*11*). Nevirapine makes contact with the side chain residues of Tyr^{181} and Tyr^{188} in the p66 subunit only. The TIBO derivatives are a structurally distinct class of inhibitors that appear to bind to the Nevirapine site (*12*), a conclusion that is supported by the observed cross-resistance of these drugs in mutant RTs (*8*, *13*). However, structural information cannot reveal which step or steps in the DNA polymerization cycle are affected by binding the inhibitor at a distant site.

Several steady-state studies have attempted to elucidate the inhibition mechanism of nonnucleoside inhibitors (*6*, *14*, *15*). In general, these studies suggest a noncompetitive inhibition pattern with respect to both primer-template and nucleotide substrates. However, the steady-state kinetic formalism does not provide an under-

R. A. Spence and K. A. Johnson are in the Department of Biochemistry and Molecular Biology, Pennsylvania State University, University Park, PA 16802, USA. W. M. Kati is with the Department of Anti-Infectives Research at the Abbott Laboratories, One Abbott Park Road, Abbott Park, IL 60064, USA. K. S. Anderson is with the Department of Pharmacology, Yale Medical School, New Haven, CT 06510, USA.

*To whom correspondence should be addressed.

standing of the mechanism of inhibition, and the kinetic analysis is complicated further by the slow release of primer template from RT in the steady state (*16*). Moreover, as shown below, inhibition leads to a change in the identity of the rate-limiting step. We now describe our analysis of three nonnucleoside inhibitors by means of pre–steady-state methods (*16–18*). Analysis of inhibition by pre–steady-state methods provides mechanistic conclusions defining elementary steps in the reaction pathway that can be related to structure directly. Our data revealed an interaction between the nucleotide site and the nonnucleoside inhibitor site, which results in inhibition of the chemical reaction.

We first examined the inhibition of HIV-1 RT by the nonnucleoside inhibitors to test the effects of the inhibitors on the kinetics of dNTP (deoxynucleoside 5′-triphosphate) binding and incorporation (*19*). Elongation of the 25·45-bp duplex DNA (25-bp primer annealed to 45-bp template) to 26·45-bp product was examined by rapid mixing of the enzyme-DNA (E·DNA) complex with the next correct nucleotide for incorporation, and analysis of the products of the polymerization reaction on a sequencing gel (*20*). In this experiment, a single nucleotide was incorporated rapidly in a "burst" of polymerization and was followed by slow steady-state release of the primer-template from the enzyme (*16, 17, 21*).

In our initial experiments, the addition of 10 to 50 μM O-TIBO at the start of the reaction provided little inhibition of the pre–steady-state burst of polymerization. However, incubation of the inhibitor with the E·DNA complex before the addition of dATP (deoxyadenosine 5′-triphosphate) to start the reaction, led to a reduction in the amplitude of the burst of polymerization (Fig. 2A). The burst rates remained independent of inhibitor concentration (22 ± 3 s^{-1}), while the amplitude of the burst phase reduced monotonically with increasing concentration of O-TIBO (Fig. 2B).

The above results suggest that the dissociation of the inhibitor from the enzyme-DNA-inhibitor (E·DNA·I) complex is slow relative to the rate of the polymerization reaction. Accordingly, the amplitude of the burst phase represents the amount of uninhibited E·DNA available for fast nucleotide incorporation in the first turnover. A fit of the data to a hyperbola provides a K_d value of 3.0 μM for formation of the E·DNA·O-TIBO complex (*22*). The K_d values for Cl-TIBO and Nevirapine were determined to be 0.2 μM and 19 nM, respectively (Table 1).

Nonnucleoside RT inhibitors bind near the proposed polymerization active site (*11, 12, 23*), which contains a triad of aspartic acid residues, namely positions 185, 186, and 110 (*24*). It is likely that Mg^{2+} is ligated to one or more of these residues during catalysis (*25, 26*). To look for possible interactions between the metal ion binding sites and the nonnucleoside inhibitor site, we examined the effect of Mg^{2+} on the binding of the inhibitors to RT. The K_d for inhibitor was measured by pre–steady-state methods as described (Fig. 2) after incubation of the E·DNA in the presence or absence of Mg^{2+}. The K_d values were 3.0

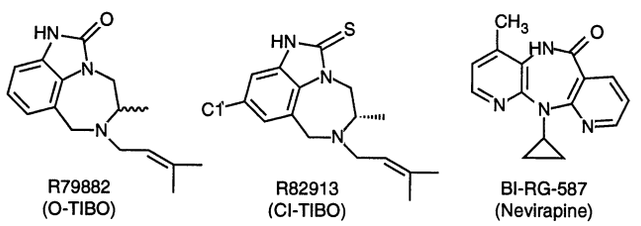

Fig. 1. Structures of HIV-1 RT specific nonnucleoside inhibitors.

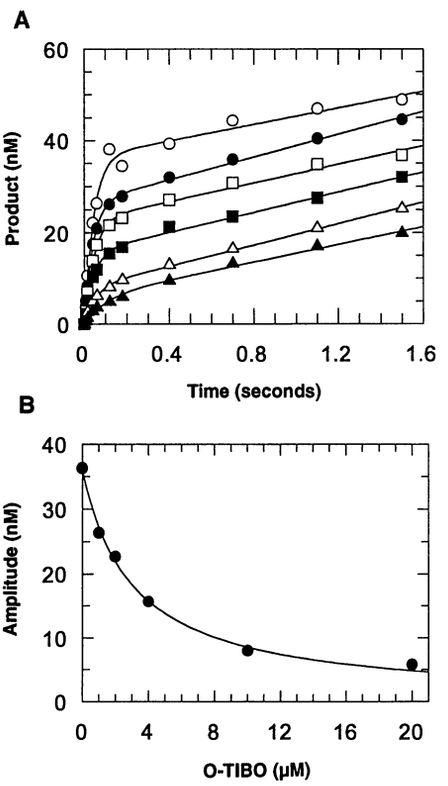

Fig. 2. Single nucleotide incorporation in the presence of O-TIBO. (**A**) RT (50 nM), (5′-^{32}P)-labeled 25·45-bp duplex DNA (100 nM), and O-TIBO were first incubated for a minimum of 20 minutes in buffer solution (50 mM tris-Cl, 50 mM NaCl, pH 7.5). This E·DNA solution was then rapidly mixed with 20 μM dATP in buffer containing 10 mM $MgCl_2$. The reactions were quenched with 0.5 M EDTA, pH 8.0 at the indicated times. The O-TIBO concentrations were 0 (○), 1.0 (●), 2.0 (□), 4.0 (■), 10.0 (△), and 20.0 (▲) μM. The concentrations are the final concentrations after 1:1 mixing in the instrument, except for O-TIBO. The O-TIBO concentrations are those of the inhibitor in the initial E·DNA solution where equilibrium is established. The individual time courses were fit to a burst equation, $y = A\cdot(1 - \exp(-kt)) + m\cdot t$. (**B**) The amplitudes of the burst phases (●) were plotted against O-TIBO concentration and fit to a hyperbolic function (solid line) to yield a K_d value of 3.0 ± 0.2 μM.

Table 1. Kinetic and equilibrium parameters for nonnucleoside inhibitors. The dissociation constants, binding rates, and dissociation rates are listed for each of the nonnucleoside inhibitors. Plus (+) or minus (−) refers to prior incubation of HIV-1 RT, DNA, and inhibitor in the presence or absence of Mg^{2+}. The values for $K_{d(dATP)}$ and the maximum rate were obtained at concentrations of inhibitor sufficient to achieve >99 percent saturation of binding.

Parameter	O-TIBO		Cl-TIBO		Nevirapine	
	−	+	−	+	−	+
K_d (μM)	3.0 ± 0.2	10.8 ± 1.1	0.21 ± 0.05	1.2 ± 0.4	0.019 ± 0.004	0.025 ± 0.01
k_{on} (10^4 M^{-1} s^{-1})	11 ± 1	5.0 ± 0.8	6.0 ± 0.5	2.0 ± 0.7	9.9 ± 0.5	2.6 ± 0.1
k_{off} (s^{-1})	0.36 ± 0.04	0.54 ± 0.09	0.013 ± 0.003	0.02 ± 0.01	0.0019 ± 0.0004	0.0007 ± 0.0003
$K_{d(dATP)}$ (μM)	0.16 ± 0.04	0.22 ± 0.08	0.13 ± 0.02	0.13 ± 0.03	<0.1	<0.1
max rate (s^{-1})	0.14 ± 0.01	0.15 ± 0.01	0.0088 ± 0.0003	0.0087 ± 0.0004	0.0087 ± 0.0009	0.0112 ± 0.0004

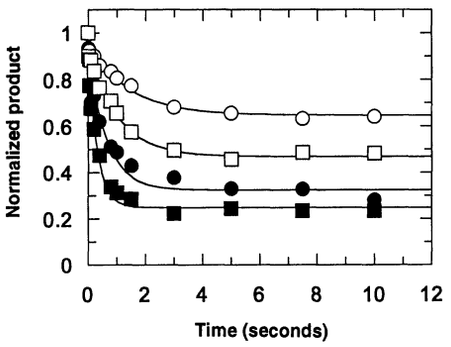

Fig. 3. The apparent binding rate of O-TIBO. RT (95 nM) was first incubated with [5′-^{32}P]-labeled DNA duplex (84 nM). This solution was rapidly mixed with an equal volume of O-TIBO at a concentration of either 10 (○,●) or 20 (□,■) μM for the indicated times, and then mixed with dATP (50 μM) for 200 ms. The reaction was quenched with 100 μl of 0.5 M EDTA (pH 8.0). The reported concentrations of RT, DNA, and O-TIBO are the concentrations after 1:1 mixing; the reported concentration of dATP is the final concentration after mixing 1:2 with the E·DNA and O-TIBO solutions. The open symbols reflect the reactions in which 10 mM Mg^{2+} had been first incubated with the enzyme-DNA and O-TIBO. The closed symbols refer to data where Mg^{2+} was present only with the nucleotide, added to initiate the reaction. In either case, the final Mg^{2+} concentration was 10 mM. The decrease in product formation with increasing incubation time reflects the binding of O-TIBO to the E·DNA complex. In reactions where Mg^{2+} was present only with the nucleotide solution, the single exponential decays gave apparent binding rates of 1.5 ± 0.3 and 3.2 ± 0.4 s^{-1} for 10 and 20 μM O-TIBO, respectively. In the reactions where Mg^{2+} was present in all the reactant syringes, the apparent binding rates were 0.7 ± 0.1 and 1.0 ± 0.1 s^{-1} for 10 and 20 μM O-TIBO, respectively.

μM in the absence and 10.8 μM in the presence of 10 mM Mg^{2+}, respectively. We observed similar results for the effect of Mg^{2+} on the equilibrium dissociation constants for Cl-TIBO and Nevirapine (Table 1). The fact that the E·DNA complex appears to have different affinities for the nonnucleoside inhibitors in the absence and presence of Mg^{2+} implies that there was an interaction between the Mg^{2+} binding site and the inhibitor binding site.

Inhibitor binding rates. Our analysis requires that the dissociation of inhibitor from the E·DNA·I complex is slow relative to the rate of polymerization. To test this assumption, the binding rates of the three nonnucleoside inhibitors were determined by means of a rapid quench-flow method entailing three sequential mixing events (*27*). First, a solution containing the E·DNA complex was rapidly mixed with the inhibitor and allowed to bind for a specified time. Second, the next correct nucleotide for incorporation, dATP, was added to the E·DNA complex to allow polymerization catalyzed by uninhibited enzyme. Third, the polymerization reaction was stopped by mixing with EDTA after 200 ms, a time sufficient to complete one enzyme turnover. In this experiment the amount of product formed in 200 ms provided a direct measurement of the concentration of uninhibited E·DNA as a function of time allowed for inhibitor binding.

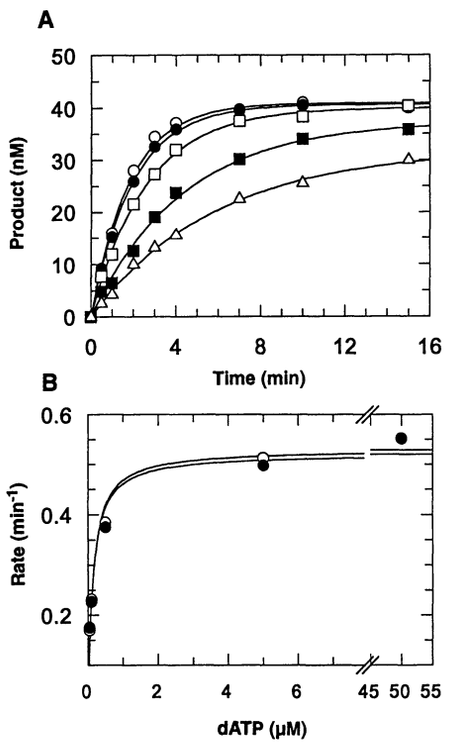

Fig. 4. The dATP concentration dependence of the nucleotide incorporation rate in the presence of saturating amounts of Cl-TIBO. (**A**) A solution of RT (50 nM), [5′-^{32}P]-labeled duplex DNA (53 nM) and 50 μM Cl-TIBO was incubated at 37°C for 15 minutes. The reaction was initiated by mixing equal volumes of Mg·dATP and E·DNA·Cl-TIBO complex solutions, and was quenched manually with 0.5 M EDTA, (pH 8.0). The concentrations reported are those obtained after 1:1 mixing of the enzyme solution with the nucleotide solution. Each of the time courses was fit to a first-order equation (solid lines). The single turnover rates increased with increasing concentrations of dATP. The dATP concentrations were 0.05 (△), 0.1 (■), 0.5 (□), 5.0 (●), and 50.0 (○) μM. (**B**) The single incorporation rates (●), as a function of the dATP concentration, were fit to a hyperbola (solid line) that corresponds to an apparent K_d value of 0.13 ± 0.02 μM and a maximum rate of incorporation of 0.0088 ± 0.0003 s^{-1} (0.53 ± 0.02 min^{-1}). Identical results were obtained when divalent magnesium was added to the buffer of the E·DNA solution (○). In both cases the final concentration of Mg^{2+} was 10 mM.

The decrease in product formed was followed as a function of the time allowed for reaction of O-TIBO with E·DNA (Fig. 3). The data were normalized to the maximum amount of turnover detected in 200 ms in the absence of inhibitor (the zero time point). Two O-TIBO concentrations (10 and 20 μM) were used, and each data set was fit to a single exponential function. At long incubation times (>3 s, in the case of O-TIBO), the E·DNA and E·DNA·O-TIBO complexes reached equilibrium, and the end points obtained from these fits agree with values calculated from the K_d (Table 1) at these concentrations of O-TIBO.

The slow binding of O-TIBO to the E·DNA complex (Fig. 3) substantiates our methods for determining both the K_d and the binding rate. Binding and dissociation rate constants for formation of the E·DNA·I complex were obtained by analysis of the concentration dependence of the observed rate of binding, where $k_{obs} = k_{on}[I] + k_{off}$. Because large errors in the extrapolated intercept did not allow an independent estimate of k_{off}, the binding rate was obtained by fitting the data to the equation $k_{obs} = k_{on}([I] + K_d)$, so that k_{off} was constrained to agree with both the K_d value and the observed binding rate (Table 1).

From the series of experiments with O-TIBO in which Mg^{2+} was added only to the nucleotide solution, k_{on} was 1.2 × 10^5 M^{-1} s^{-1} and k_{off} was 0.36 s^{-1}. Prior incubation of the metal ion with the enzyme-DNA solution decreased the rate of inhibitor binding (k_{on} = 5.0 × 10^4 M^{-1} s^{-1}) but did not significantly affect its dissociation rate (k_{off} = 0.54 s^{-1}). The association and dissociation rates of Cl-TIBO and Nevirapine were determined in a similar manner and the values are recorded in Table 1. Because the inhibitors bind faster than the DNA dissociates from RT (0.2 s^{-1}), the inhibitors are capable of binding to the E·DNA complex.

At concentrations of inhibitor sufficient to eliminate the fast burst of polymerization, there was only slight inhibition of the slow, linear phase of polymerization (Fig. 2A). Measurements in the steady state showed that the rate was only decreased from a value of 0.26 s^{-1} in the absence of inhibitor to a value of 0.11 s^{-1} at 20 μM O-TIBO. Thus, even at saturating concentrations of inhibitor, a slow but significant reaction continued. This continued polymerization reaction suggests that the E·DNA·I complex is capable of binding dNTP and catalyzing polymerization at a finite, but slower rate. Analysis of the effect of increasing inhibitor concentration on this slow polymerization established that the observed reaction was due to catalysis by the fully inhibited enzyme and not due to the slow release of inhibitor with subsequent catalysis of the uninhibited enzyme.

Nucleotide binding to E·DNA·I. Single turnover experiments were performed to examine the dATP concentration dependence of the rate of the slow polymerization reaction in the presence of saturating concentrations of inhibitor (*28*). The inhibitor was added to the preformed E·DNA complex, and this solution was then mixed with an equal volume of a dATP solution to initiate the polymerization; the complete reaction mixture was then sampled at various times and quenched. The rates of product formation in the presence of >99 percent saturation of Cl-TIBO or Nevirapine were slow enough to be measured by manually quenching the reactions; however, the "rapid quench" apparatus was needed in experiments with O-TIBO because of the faster polymerization rate catalyzed by the enzyme inhibited by O-TIBO. The concentration of 26-bp product was plotted as a function of time of polymerization catalyzed by RT that had been incubated with 50 μM Cl-TIBO before the addition of dATP (Fig. 4A). Equilibrium between the inhibitor and the E·DNA complex was established in these solutions before the mixing with nucleotide, and nearly all (99.6 percent) of the E·DNA sites were bound by the inhibitor at the concentrations of RT and Cl-TIBO that were used. Each time course was fit to a single exponential to obtain the rate of reaction at each dATP concentration. A plot of incorporation rate as a function of dATP concentration (Fig. 4B) was fit to a hyperbola, which gave a maximum rate of dATP incorporation of 0.0088 s^{-1} (0.53 min^{-1}) and an apparent K_d for dATP binding of 0.13 μM. This result was surprising, and it suggested that the binding of dATP to E·DNA was 40 times tighter when the inhibitor was present compared to a K_d of 5 μM for dATP in the absence of inhibitor (*16*). We can now understand this result in terms of the two-step nucleotide binding, as shown below.

Identical results were obtained when Mg^{2+} was added to the buffers of both the E·DNA and nucleotide solutions before they were mixed to initiate the reaction (Fig. 4B). This observation was expected because on this slow time scale the metal ion equilibrated with the E·DNA·I complex even when the ion was added only to the nucleotide solution. For Nevirapine, there was no significant reduction in rate when the nucleotide concentrations were lowered within the range of concentrations that could be used relative to the enzyme concentration. Because of the limitations of the minimal protein and DNA concentrations necessary to perform the experiment, the apparent K_d of dATP in the presence of saturating Nevirapine is reported as an upper limit (Table 1).

If the observed slow reaction was due to catalysis by the fully inhibited complex (E·DNA·I) then the low K_d for dATP was simply due to the tighter binding of the nucleotide in the presence of inhibitor. Alternatively, the observed tighter binding could be explained by a model invoking dissociation of the inhibitor from the enzyme at a slow rate followed by fast dATP binding and catalysis from the free E·DNA complex. According to this model, the rate of turnover would be limited by the rate of inhibitor release and the apparent K_d for dATP would be a function of the kinetic partitioning of free E·DNA between dATP binding and inhibitor rebinding. The apparent K_d for dATP should then be a function of inhibitor concentration, at concentrations above those required to saturate the enzyme sites with inhibitor (*29*). Several experiments were performed to determine whether the apparent K_d for dATP or the maximum rate of nucleotide incorporation changed with inhibitor concentration. When the E·DNA complex was >99 percent saturated with O-TIBO, the maximum rate of incorporation and apparent K_d were 0.14 s^{-1} and 0.16 μM, respectively (Table 1). At lower concentrations of O-TIBO, the data were fit to a first-order rate plus an initial offset, which we attribute to the rapid burst of reaction catalyzed by the fraction of E·DNA complex not bound to inhibitor. The maximum rates of single turnover and the apparent K_d in the presence of 15 μM O-TIBO (about 82 percent saturation) and 40 μM O-TIBO (about 93 percent saturation) were both similar to those obtained when E·DNA was >99 percent saturated. The fact that the apparent K_d did not change with varying O-TIBO concentration implies that the observed slow phase of reaction is due to catalysis by the E·DNA·I complex, and not to catalysis by E·DNA after slow release of inhibitor. Accordingly, the tight dATP binding must be a function of the interaction of the nucleotide with the E·DNA·I complex. This tight binding can be understood on the basis of the two-step nucleotide binding sequence provided that the inhibitors act by slowing the rate of the chemical reaction.

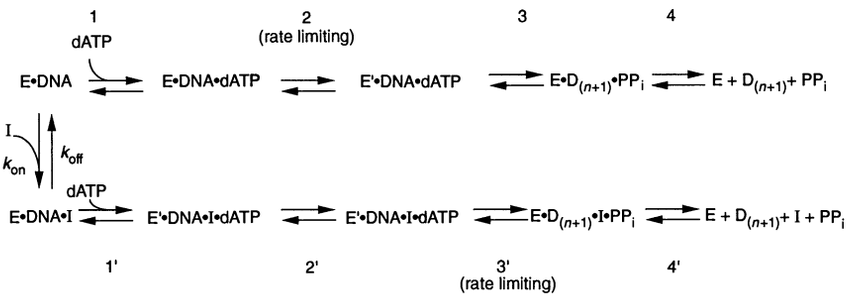

Scheme 1

Mechanism of inhibition. Previous reports regarding the mechanism of action of these inhibitors have suggested that the inhibitors act noncompetitively with respect to the incoming nucleotide, which might result from inhibition of the conformational change required for catalysis, from inhibition of the chemical reaction per se, from inhibition of product release, or as a result of a change in the rate-limiting step during steady-state catalysis. Pre–steady-state studies of DNA polymerization catalyzed by RT, in the presence of nonnucleoside inhibitors, now lead to the conclusion that these inhibitors act by slowing the rate of the chemical reaction catalyzed by RT (Scheme 1). The slow chemical reaction allows the two-step binding of dNTP to come to equilibrium leading to tighter binding of the nucleotide.

Our results quantify the tight binding of Nevirapine, O-TIBO, and Cl-TIBO, to the E·DNA complex. The observed reduction in burst amplitude when the inhibitor was first incubated with the E·DNA complex permitted a direct determination of the amount of uninhibited E·DNA available for fast incorporation. The inhibitor dissociation constants were measured with the use of a model dependent on the slow equilibration of the inhibitor with the E·DNA complex, and this model was supported by direct measurements of the binding rates. Under the conditions of our assays, the inhibitor binding rates to the E·DNA complex were approximately two orders of magnitude slower than the rate of binding of correct nucleotide. These slow binding characteristics have also been described for a pyridinone nonnucleoside inhibitor (*23*) and, in previous studies, the slow binding rate has been attributed to competition of Cl-TIBO with the primer-template for binding RT, suggesting that efficient binding of inhibitor requires DNA release (*30*). As with many "slow" binding inhibitors, the second-order rate constant for inhibitor binding is not what governs the observed slow binding. Rather, it is the slow dissociation rate that leads to slow binding kinetics at concentrations of inhibitor sufficient to saturate the equilibrium binding. Moreover, analysis of inhibitor binding kinetics (Fig. 3) demonstrates that at high concentrations the inhibitors bind at rates faster

than the slow DNA release from RT (0.2 s^{-1}). Therefore, in contrast to previous conclusions, DNA release is not required for inhibitor binding to the enzyme.

The presence of magnesium ions bound to the E·DNA complex weakens the binding of the nonnucleoside inhibitors. Although a crystal structure of RT has not been solved in which a metal ion or ions are ligated to residues in the proposed polymerase active site, we should consider the role and locations of these ions during catalysis. Three aspartic acid residues in a highly conserved region for polymerases (*31*) have been proposed to participate in catalytic activity (*32*). At least two Mg^{2+} ions may be assisting with polymerization by ligating to the carboxyl groups of these aspartic acids (*26*). Nevirapine binds near the β turn containing Asp^{185} and Asp^{186} (*11*). TIBO competition studies and inference from cross-resistant RT mutants suggest that the TIBO derivatives bind to RT in the same region as Nevirapine.

As a result of incubation of the E·DNA·I complex with Mg^{2+}, the K_d values for O-TIBO and Cl-TIBO were 3.5 and 6 times higher, respectively. Although we did not observe a significant effect of Mg^{2+} on the K_d for Nevirapine, it is possible that the extremely low K_d value for Nevirapine binding made it difficult to measure accurately a significant change in the K_d when the E·DNA complex was incubated with Mg^{2+}. Alternatively, it is possible that the TIBO class of inhibitors contain a distinct functional group that is hindered upon binding to Mg·E·DNA relative to free E·DNA. Prior incubation of Mg^{2+} with E·DNA caused a decrease (two to three times lower) in the rates of binding of the three inhibitors (Table 1). It is possible that carboxyl groups sitting above the binding pocket ligated to Mg^{2+} ion or ions impede the incoming route for the inhibitor to bind RT, and that once the inhibitor is bound only the affinity to the enzyme itself dictates the dissociation rate.

Our results provide direct evidence for communication between the inhibitor site and the catalytic site. Because Mg^{2+} affects the K_d values of the inhibitors, it is plausible that binding of inhibitor alters the positions of the carboxyl ligands so as to significantly slow the rate of the Mg^{2+}-dependent chemical reaction. On the basis of the crystal structure of Nevirapine-bound RT (*11*), the inhibitor was described as being "adjacent to but not overlapping the proposed polymerization active site". We have shown that when nonnucleoside inhibitor is bound RT still carries out catalysis, albeit, at a slow rate (Fig. 4A).

The parameters summarized in Table 1 can be understood by considering scheme 1, where the inhibitors act by slowing the rate of the chemical reaction in the E·DNA·I·dATP complex. The apparent tight binding of dATP to form this complex, with a K_d value of about 130 nM, was unexpected. This value implies that nucleotide binding is 40 times tighter than that of the ground-state K_d of 5 μM measured in a single turnover experiment in the absence of inhibitor (*16*). These results can be analyzed in terms of the two-step nucleotide binding mechanism. In the absence of inhibitor, the correct dNTP binds initially in the ground state, with a K_d of approximately 5 μM. This ground-state binding is followed by a rate-limiting conformational change that is then followed by the chemical reaction. We have recently measured the equilibrium constant for the two-step nucleotide binding (*33*). If the chemical reaction is prevented, the dissociation constant for the two-step nucleotide binding is approximately 20 nM, indicating a dimensionless equilibrium constant of 280 for the conformational change. Because the conformational change is rate-limiting in the absence of inhibitor, the single turnover experiments provide a measurement of the K_d of only the ground-state collision complex (Scheme 1, step 1). However, if the chemical reaction is rate-limiting in the presence of inhibitor, the single turnover experiments examining the dATP concentration dependence of the incorporation rates provide a measure of the overall K_d including both steps which equilibrate on the time scale leading up to the rate-limiting step of the reaction. Thus, the observed K_d of 130 nM seen in the presence of the nonnucleoside inhibitor should be compared to the overall K_d of 20 nM, an indication that the binding of dATP is six times weaker. Accordingly, the inhibitors do not significantly alter the equilibrium constants for nucleotide binding. Fluorescence titrations to determine directly the K_d for nucleotide binding to the E·DNA complex in the presence of saturating amounts of inhibitor (*33*) gave values of the apparent K_d similar to our results, further supporting our model of slow catalysis by the inhibited enzyme.

Taken together, the observed tight binding of dATP, along with the lack of any effect of inhibitor concentration on the rate of turnover and the apparent K_d for dATP, supports the conclusion that the nonnucleoside inhibitors slow the rate of the chemical reaction, but do not significantly alter the rate or equilibrium constant for the conformational change. Although the rate of the conformational change could be slowed somewhat, it is not rate-limiting in the presence of inhibitor.

We propose that when these nonnucleoside inhibitors bind to the E·DNA complex, the chemical step for incorporation of correct nucleotide becomes the rate-limiting step of the pathway, rather than the conformational change that determines the fast rate of incorporation for the uninhibited enzyme. Scheme 1 demonstrates the complete mechanism of RT in the presence of these nonnucleoside inhibitors. The results obtained with Mg^{2+} bound to E·DNA before the addition of the substrate allow us to consider the communication between the catalytic active site and the inhibitor binding pocket. We have shown that there is a measurable interaction between the nonnucleoside inhibitors and the catalytically required Mg^{2+} whereby the affinity of the inhibitor for the E·DNA complex is reduced in the presence of the metal ion. Another consequence of this interaction can be realized in the slow catalytic rate of E·DNA·I. The likelihood that Mg^{2+} ions ligate to the carboxyl groups of the conserved aspartic acid residues, and the fact that Nevirapine (and presumably TIBO) binds near these residues, suggest that the E·DNA·I complex permits the two-step binding of nucleotide where the Mg^{2+} ions are not in proper alignment with the carboxyl groups for efficient catalysis. Binding of the nucleotide to the E·DNA·I complex, although tight, is not utilized efficiently to promote catalysis.

We have established the mechanism of inhibition of RT by the three nonnucleoside inhibitors. Although the long-term inhibition of RT is limited by the high frequency of mutations of the enzyme, this detailed understanding of the action taken by RT when presented with these inhibitors should assist in the search for effective drugs to attenuate the AIDS virus. In particular, the interaction between the nucleotide binding site and the nonnucleoside inhibitor site may provide a means to increase the effectiveness of drugs used in combination therapy. A single drug combining the functionalities of a nucleotide analog and a nonnucleoside inhibitor would bind much more tightly because of the cooperative interactions between the sites.

REFERENCES AND NOTES

1. E. De Clercq, *Biochem. Pharmacol.* **47**, 155 (1994); S. P. Goff, *J. Acquired Immune Defic. Syndr.* **3**, 817 (1990); A. Jacobo-Molina *et al.*, *Proc. Natl. Acad. Sci. U.S.A.* **90**, 6320 (1993); H. Mitsuya, R. Yarchoan, S. Broder, *Science* **249**, 1533 (1990).
2. D. Richman *et al.*, *Antimicrob. Agents Chemother.* **35**, 305 (1991); R. Yarchoan, H. Mitsuya, C. E. Myers, S. Broder, *N. Engl. J. Med.* **321**, 726 (1989).
3. B. A. Larder and S. D. Kemp, *Science* **246**, 1155 (1989).
4. The three nonnucleoside inhibitors examined were: O-TIBO, ((±)-4,5,6,7-tetrahydro-5-methyl-6-(3-methyl-2-butenyl)-imidazo[4,5,1-*jk*][1,4]-benzodiazepin-2(1*H*)-one); Cl-TIBO; (+)-*S*-4,5,6,7-tetrahydro-9-chloro-5-methyl-6-(3-methyl-2-butenyl)-imidazo [4,5,1-*jk*][1,4]-benzodiazepin-2(1*H*)-thione; and Nevirapine, 11-cyclopropyl-5,11-dihydro-4-methyl-6*H*-dipyrido [3,2-*b*:2′,3′-*e*] [1,4] diazepin-6-one.
5. R. Pauwels *et al.*, *Nature* **343**, 470 (1990).
6. V. J. Merluzzi *et al.*, *Science* **250**, 1411 (1990).
7. B. A. Larder, G. Darby, D. D. Richman, *ibid.* **243**,

1731 (1989); D. D. Richman, J. M. Grimes, S. W. Lagakos, *J. Acquired Immune Defic. Syndr.* **3**, 743 (1990).
8. J. W. Mellors *et al.*, *Mol. Pharmacol.* **41**, 446 (1992); J. H. Nunberg *et al.*, *J. Virol.* **65**, 4887 (1991); D. Richman *et al.*, *Proc. Natl. Acad. Sci. U.S.A.* **88**, 11241 (1991).
9. J. W. Mellors *et al.*, *Mol. Pharmacol.* **43**, 11 (1993); D. D. Richman *et al.*, *J. Virol.* **68**, 1660 (1994).
10. T. J. Dueweke *et al.*, *Proc. Natl. Acad. Sci. U.S.A.* **90**, 4713 (1993); B. A. Larder, *Antimicrob. Agents Chemother.* **36**, 2664 (1992); M. H. St. Clair *et al.*, *Science* **253**, 1557 (1991).
11. L. A. Kohlstaedt, J. Wang, J. M. Friedman, P. A. Rice, T. A. Steitz, *Science* **256**, 1783 (1992).
12. J. C. Wu *et al.*, *Biochemistry* **30**, 2022 (1991).
13. J. Balzarini *et al.*, *Virology* **192**, 246 (1993).
14. I. W. Althaus *et al.*, *J. Biol. Chem.* **268**, 6119 (1993); Z. Debyser *et al.*, *Proc. Natl. Acad. Sci. U.S.A.* **88**, 1451 (1991); K. B. Frank, G. J. Noll, E. V. Connell, I. S. Sim, *J. Biol. Chem.* **266**, 14232 (1991); M. E. Goldman *et al.*, *Proc. Natl. Acad. Sci. U.S.A.* **88**, 6863 (1991); P. B. Taylor *et al.*, *J. Biol. Chem.* **269**, 6325 (1994); E. Tramontano and Y.-C. Cheng, *Biochem. Pharmacol.* **43**, 1371 (1992).
15. S. S. Carroll *et al.*, *J. Biol. Chem.* **268**, 276 (1993).
16. W. M. Kati, K. A. Johnson, L. F. Jerva, K. S. Anderson, *ibid.* **267**, 25988 (1992).
17. K. A. Johnson, *Enzymes* **20**, 1 (1992).
18. M. J. Donlin, S. S. Patel, K. A. Johnson, *Biochemistry* **30**, 538 (1991); S. S. Patel, I. Wong, K. A. Johnson, *ibid.*, p. 511; I. Wong, S. S. Patel, K. A. Johnson, *ibid.*, p. 526; K. S. Anderson, J. A. Sikorski, K. A. Johnson, *ibid.* **27**, 7395 (1988).
19. HIV-1 reverse transcriptase was purified as described (*16*) from a clone expressing both p51 and p66 [B. Muller *et al.*, *J. Biol. Chem.* **264**, 13975 (1989)]. The protein concentration was determined spectrophotometrically at 280 nm, with the extinction coefficients 136,270 and 124,180 M^{-1} cm^{-1} for the 66- and 51-kD subunits, respectively. The preparation gave a reaction amplitude of approximately 0.45 site per p66 or p51 heterodimer. On the basis of an active site titration all enzyme concentrations were corrected for the fraction of active protein. A synthetic DNA duplex 25·45-bp (*16*) was used in which the next correct base for incorporation was dATP. Concentrations of the oligonucleotides were estimated by ultraviolet absorbance at 260 nm with calculated extinction coefficients for 25 bp, ε = 249,040 M^{-1} cm^{-1}; and for 45 bp, ε = 491,960 M^{-1} cm^{-1}. Before annealing, the primer was 5′-labeled with T4 polynucleotide kinase and [γ-^{32}P]ATP.
20. Experiments to measure polymerization kinetics were performed as described (*16*). Rapid quench experiments were done with a previously designed apparatus [K. A. Johnson, *Methods Enzymol.* **134**, 677 (1986)] (built by KinTek Corporation, State College, PA). Typically, the experiments were done by first allowing the RT and duplex DNA to incubate in reaction buffer (50 mM tris-Cl, 50 mM NaCl, pH 7.5) either in the presence or absence of 10 mM $MgCl_2$. A sample of this solution (15 μl) was rapidly mixed with an equal volume of a solution of substrate and allowed to react for specified times. The reactions were terminated by quenching with approximately 80 μl of 0.5 M EDTA at pH 8.0. All reactions were performed at 37°C. Unless noted otherwise, all concentrations mentioned refer to concentrations during the reaction after mixing. Single nucleotide incorporation was monitored by extension of (5′-^{32}P)-labeled 25-bp to 26-bp oligo-nucleotides. The products were resolved from starting material on a denaturing polyacrylamide gel (16 to 20 percent), and the dried gel was scanned with a Betascope 603 blot analyzer (Betagen, Waltham, MA). Data were fit by nonlinear regression with the use of program GraFit (Erithacus Software, Staines, UK). The pre–steady-state burst experiments (Fig. 2A) were fit to the burst equation: $y = A\cdot(1-\exp(-kt) + m\cdot t$, where A represents the burst amplitude; k, the burst rate; and m, the slope of the linear phase. The steady-state rate is calculated by dividing the slope by the concentration of total active enzyme.
21. K. A. Johnson, *Annu. Rev. Biochem.* **62**, 685 (1993).
22. The equilibrium dissociation constants determined for O-TIBO (Fig. 2B) were derived from hyperbolic fits to the data. The K_d values for Cl-TIBO and Nevirapine were small relative to the enzyme concentration; these data, therefore, had to be fit to a quadratic equation: $y = E_O - 0.5\cdot\{(K_d + E_O + I_o) - [(K_d + E_O + I_o)^2 - 4\cdot E_O\cdot I_o]^{1/2}\}$ where y represents the uninhibited E·DNA complex, E_0 is the total enzyme concentration, I_0 is the total inhibitor concentration, and K_d is the equilibrium dissociation constant for the nonnucleoside inhibitor.
23. K. A. Cohen *et al.*, *J. Biol. Chem.* **266**, 14670 (1991).
24. L. Ratner *et al.*, *Nature* **313**, 277 (1985).
25. D. M. Lowe, V. Parmar, S. D. Kemp, B. A. Larder, *FEBS Lett.* **282**, 231 (1991).
26. H. Pelletier, M. R. Sawaya, A. Kumar, S. H. Wilson, J. Kraut, *Science* **264**, 1891 (1994); T. A. Steitz, *Curr. Opin. Struct. Biol.* **3**, 31 (1993).
27. The apparent rate of inhibitor binding was obtained by mixing the E·DNA complex with a given concentration of nonnucleoside inhibitor for specified times. By loading the next correct nucleotide into a third syringe, the time course of inhibitor binding could be assayed by reaction with nucleotide substrate for a time sufficient to complete one turnover (200 ms). A modification of the rapid quench apparatus allowed for this second delay, holding all reactants in the instrument for the 200-ms incubation. The reaction mixture was then expelled from the instrument into 100 μl of 0.5 M EDTA (pH 8.0) to terminate the reaction. The reported concentrations of RT, DNA, and O-TIBO are the concentrations after 1:1 mixing; the reported concentration of dATP is the final concentration after mixing 1:2 with the E·DNA and O-TIBO solutions. The product DNA concentrations were normalized by the maximum amount of turnover seen in 200 ms (the amount of product formed in 200 ms in the absence of inhibitor). The data were fit to a single exponential decay plus a constant ($y = A\cdot\exp(-k_{obs}\cdot t) + C$) where A is equal to the difference in the burst amplitudes of polymerization catalyzed by E·DNA and E·DNA partially saturated with inhibitor, k_{obs} is the observed rate of inhibitor binding, and C reflects the burst amplitude of the equilibrium mixture obtained between the inhibitor and the E·DNA complex.
28. RT and duplex DNA were first incubated for 10 to 15 minutes, and then saturating amounts (five times the K_d) of the nonnucleoside inhibitor were added and the mixture was incubated for an additional 10 to 15 minutes. The reaction was initiated by the addition of equal volumes of Mg·dATP and the E·DNA·I solutions. Small portions of the reacting solution (5 μl) were quenched by mixing with 15 μl of 0.5 M EDTA (pH 8.0) at the specified times. The reactions were repeated with increasing concentrations of dATP. For experiments with O-TIBO, the rapid chemical quench instrument had to be used because of the faster reaction rate. A single exponential was used to fit the time courses for each dATP concentration (Fig. 4A), $y = A\cdot(1 - \exp(-k\cdot t))$. For experiments where the fraction of inhibitor saturation was not >99 percent, a constant was added to the first-order equation to account for fast turnover by any uninhibited E·DNA complex present. That is, the data were fit to an equation of the form, $y = A\cdot(1 - \exp(-k\cdot t)) + C$, where C represents the amplitude of the fast reaction catalyzed by the small fraction of uninhibited enzyme. This analysis allowed the measurement of the rate of the slow reaction catalyzed by the inhibited enzyme species even in the presence of a fraction of uninhibited enzyme.
29. A model was considered where the inhibition mechanism involves simple, reversible binding of the inhibitor to the E·DNA complex and any polymerization observed is strictly from uninhibited RT due to the slow release of inhibitor followed by rapid binding of dNTP to the uninhibited enzyme. This model is like Scheme 1 except that steps 1′, 2′, 3′, and 4′ involving reaction of inhibited enzyme are precluded. According to this model, the single turnover rates measured in the presence of saturating amounts of inhibitor can be represented by the expression $k_{obs} = k_{off}$ [dATP]/([dATP] + k_{on}[I]/k_1). In this equation k_{obs} is the first-order rate constant for single nucleotide incorporation in the presence of a saturating concentration of inhibitor (Fig. 4A); k_{off} refers to the dissociation rate of inhibitor from E·DNA, and k_{on} and k_1 are the binding rates of inhibitor and nucleotide to E·DNA, respectively, as in Scheme 1. The observed rate, k_{obs} is a product of the inhibitor dissociation rate and the partitioning of the free E·DNA complex to rebind inhibitor or incorporate nucleotide, and the term k_{on}[I]/k_1 represents the apparent K_d for dATP. These equations suggest a linear relationship between the apparent K_d for dATP and the inhibitor concentration. However, the apparent dissociation constants of dATP obtained from these experiments were independent of inhibitor concentration at concentrations ranging from 5 to 170 times the K_d for the inhibitor. These results imply that the observed slow reaction must be due to catalysis by the E·DNA·I complex and not attributable to fast catalysis by E·DNA following slow release of inhibitor from E·DNA·I.
30. V. Gopalakrishnan and S. Benkovic, *J. Biol. Chem.* **269**, 4110 (1994).
31. M. Delarue, V. Pock, N. Tordo, D. Moras, P. Argos, *Protein Eng.* **3**, 461 (1990).
32. B. A. Larder, D. J. M. Purifoy, K. L. Powell, G. Darby, *Nature* **327**, 716 (1987).
33. K. Rittinger *et al.*, in preparation.
34. We thank B. Muller and R. Goody for providing the clone expressing HIV p51 and p66. Supported by NIH grants GM44613 (K.A.J.) and GM49551 (K.S.A.).

19 July 1994; accepted 23 December 1994